

## Effects of substrate stress and light intensity on enhanced biological phosphorus removal in a photo-activated sludge system

Mohamed, A. Y.A.; Welles, L.; Siggins, A.; Healy, M. G.; Brdjanovic, D.; Rada-Ariza, A. M.; Lopez-Vazquez, C. M.

**DOI**

[10.1016/j.watres.2020.116606](https://doi.org/10.1016/j.watres.2020.116606)

**Publication date**

2021

**Document Version**

Final published version

**Published in**

Water Research

**Citation (APA)**

Mohamed, A. Y. A., Welles, L., Siggins, A., Healy, M. G., Brdjanovic, D., Rada-Ariza, A. M., & Lopez-Vazquez, C. M. (2021). Effects of substrate stress and light intensity on enhanced biological phosphorus removal in a photo-activated sludge system. *Water Research*, 189, Article 116606. <https://doi.org/10.1016/j.watres.2020.116606>

**Important note**

To cite this publication, please use the final published version (if applicable). Please check the document version above.

**Copyright**

Other than for strictly personal use, it is not permitted to download, forward or distribute the text or part of it, without the consent of the author(s) and/or copyright holder(s), unless the work is under an open content license such as Creative Commons.

**Takedown policy**

Please contact us and provide details if you believe this document breaches copyrights. We will remove access to the work immediately and investigate your claim.



# Effects of substrate stress and light intensity on enhanced biological phosphorus removal in a photo-activated sludge system

A.Y.A. Mohamed<sup>a,b,c,\*</sup>, L. Welles<sup>a</sup>, A. Siggins<sup>b</sup>, M.G. Healy<sup>b</sup>, D. Brdjanovic<sup>a,d</sup>,  
A.M. Rada-Ariza<sup>a</sup>, C.M. Lopez-Vazquez<sup>a</sup>

<sup>a</sup> Environmental Engineering and Water Technology Department, IHE Delft Institute for Water Education, Westvest 7, 2611 AX Delft, The Netherlands

<sup>b</sup> Civil Engineering and Ryan Institute, College of Science and Engineering, NUI Galway, Republic of Ireland

<sup>c</sup> Animal and Grassland Research and Innovation Centre, Teagasc, Moorepark, Fermoy, Co. Cork, Ireland

<sup>d</sup> Department of Biotechnology, Delft University of Technology, Van der Maasweg 9, 2629 HZ, Delft, the Netherlands



## ARTICLE INFO

### Article history:

Received 23 May 2020

Revised 3 November 2020

Accepted 4 November 2020

Available online 6 November 2020

### Keywords:

Enhanced biological phosphorus removal

Poly-phosphate accumulating organisms

Photo activated sludge

Microalgae

PAOs-microalgae symbiosis

## ABSTRACT

Photo-activated sludge (PAS) systems are an emerging wastewater treatment technology where microalgae provide oxygen to bacteria without the need for external aeration. There is limited knowledge on the optimal conditions for enhanced biological phosphorus removal (EBPR) in systems containing a mixture of polyphosphate accumulating organisms (PAOs) and microalgae. This research aimed to study the effects of substrate composition and light intensity on the performance of a laboratory-scale EBPR-PAS system. Initially, a model-based design was developed to study the effect of organic carbon (COD), inorganic carbon ( $\text{HCO}_3^-$ ) and ammonium-nitrogen ( $\text{NH}_4\text{-N}$ ) in nitrification deprived conditions on phosphorus (P) removal. Based on the mathematical model, two different synthetic wastewater compositions ( $\text{COD}:\text{HCO}_3^-:\text{NH}_4\text{-N}$ : 10:20:1 and 10:10:4) were examined at a light intensity of  $350 \mu\text{mol m}^{-2} \text{sec}^{-1}$ . Add to this, the performance of the system was also investigated at light intensities: 87.5, 175, and  $262.5 \mu\text{mol m}^{-2} \text{sec}^{-1}$  for short terms. Results showed that wastewater having a high level of  $\text{HCO}_3^-$  and low level of  $\text{NH}_4\text{-N}$  (ratio of 10:20:1) favored only microalgal growth, and had poor P removal due to a shortage of  $\text{NH}_4\text{-N}$  for PAOs growth. However, lowering the  $\text{HCO}_3^-$  level and increasing the  $\text{NH}_4\text{-N}$  level (ratio of 10:10:4) balanced PAOs and microalgae symbiosis, and had a positive influence on P removal. Under this mode of operation, the system was able to operate without external aeration and achieved a net P removal of  $10.33 \pm 1.45 \text{ mg L}^{-1}$  at an influent COD of  $100 \text{ mg L}^{-1}$ . No significant variation was observed in the reactor performance for different light intensities, indicating the EBPR-PAS system can be operated at low light intensities with a positive influence on P removal.

© 2020 The Authors. Published by Elsevier Ltd.

This is an open access article under the CC BY license (<http://creativecommons.org/licenses/by/4.0/>)

## 1. Introduction

Removal of phosphorus (P) from wastewaters before discharge is essential to mitigate negative environmental impacts. This can be achieved either chemically or biologically, although biological removal, via enhanced biological phosphorus removal (EBPR) in activated sludge systems, is effective in achieving higher P removal efficiencies at lower operational costs than chemical alternatives (Bashar et al., 2018). In the conventional EBPR process, mixed liquor is recirculated through alternating anaerobic-aerobic stages to promote the growth of poly-phosphate accumulating organisms (PAOs). In the anaerobic stage, PAOs take up volatile fatty

acids (VFAs) present in the influent and store them as poly- $\beta$ -hydroxyalkanoates (PHA), using glycogen as a reducing agent, and obtain the required energy through the hydrolysis of intracellularly stored poly-phosphates (poly-P) (Wentzel et al., 2008). The hydrolysis of poly-P results in the anaerobic release of ortho-phosphate ( $\text{PO}_4\text{-P}$ ) into the bulk liquid. In the aerobic stage, PAOs oxidize the PHA, obtaining energy for replenishing glycogen for growth and  $\text{PO}_4\text{-P}$  uptake (Wentzel et al., 2008). In sum, the oxygen ( $\text{O}_2$ ) required by the EBPR process is usually supplied by mechanical aeration, which may increase the operational costs of aeration, and contribute up to 45–75 % of the total energy costs of activated sludge systems (Rosso et al., 2008).

In this context, photosynthetic oxygen generation by microalgae has been utilized for wastewater treatment in the presence of natural or artificial lighting (e.g. wastewater stabilization ponds

\* Corresponding author.

E-mail address: [a.yosif@hotmail.com](mailto:a.yosif@hotmail.com) (A.Y.A. Mohamed).

(WSP) and high rate algal ponds (HRAP); Craggs et al., 2014). However, these systems require a large surface area, and may have poor a nutrient removal capacity when compared to conventional activated sludge systems (Craggs et al., 2003; Mara, 2004; Sutherland et al., 2014). The recent development of photo-activated sludge (PAS) systems at laboratory-scale aims to exploit the synergetic benefits of microalgae and activated sludge systems (Abouhend et al., 2018; Ahmad et al., 2017). In this process, microalgae and bacteria co-exist in flocs or granules in a symbiotic relationship that allows for exchange of carbon dioxide ( $\text{CO}_2$ ) and  $\text{O}_2$ . In addition to oxidation of organic matter (OM) and nitrification, microalgal-bacterial flocs can also assimilate nitrogen (N), P, and OM in large quantities for growth (Manser et al., 2016; Rada-Ariza et al., 2017; Ji et al., 2020a). Furthermore, PAS systems at the laboratory-scale have been shown to improve biomass settleability of microalgae, enhance solid-liquid separation (Ji et al., 2020a), and reduce the system's  $\text{CO}_2$  footprint (Anbalagan et al., 2017).

The development of PAOs in PAS systems may also improve biological P removal (Carvalho et al., 2018). Furthermore, the intracellular poly-P stored by PAOs may increase the density and settleability of the microalgae-bacteria flocs (Schuler et al., 2001). Carvalho et al. (2018) developed a laboratory-scale EBPR-PAS system and attained higher P removal efficiency ( $79 \pm 8\%$ ) without external aeration, at a low influent chemical oxygen demand (COD)/P ratio. However, from the perspective of design parameters, the interaction between PAOs and microalgae is not fully understood (Carvalho et al., 2018). There are significant knowledge gaps regarding the effect of substrate composition and light intensity on EBPR in systems containing a mixture of PAOs and microalgae. Wastewater composition and solar radiation can demonstrate substantial variability, both temporally and spatially (Henze and Comeau, 2008; EUMETSAT, 2020), therefore, a better understanding of the influence of these parameters is important for the further development of EBPR-PAS systems.

Thus, to address this knowledge gap, a stoichiometric EBPR-PAS model-based design was first investigated to understand the impact of carbon (C) and N on P removal. Following the model development, two different synthetic wastewater compositions of COD: $\text{HCO}_3^-$ : $\text{NH}_4\text{-N}$  of 10:20:1 and 10:10:4 were examined in controlled laboratory reactor experiments to evaluate P removal. In addition, the short-term effects of four incident light intensities (350, 262.5, 175, and  $87.5 \mu\text{mol m}^{-2} \text{sec}^{-1}$ ), were also investigated to evaluate the stability of symbiotic PAOs-microalgal capacity for P removal.

## 2. Materials and Methods

### 2.1. Model-based design

Prior to the start-up, a model-based design approach was used to identify the theoretically optimal operating conditions (including synthetic wastewater composition, light intensity, and operational and environmental conditions). The model (Tables A.1 to A.3, Appendix A of the Supplementary Information) was developed in MS Excel<sup>TM</sup> using the EBPR stoichiometric-based, steady-state design model developed by Comeau et al. (1986), Wentzel et al. (1990), and Smolders et al. (1994a,b). This model was modified and extended by coupling the oxygen requirements of the aerobic EBPR activity to the oxygen generation by microalgae (Mara, 2004).

To develop the model, the following assumptions were made: a) operation of an EBPR-PAS system in a completely mixed sequencing batch reactor (SBR) (Wilderer et al., 2001) under alternating anaerobic-aerobic EBPR conditions, with dark conditions during the anaerobic stage and illuminated conditions during the aerobic stage; b) operation of the EBPR-PAS system with a total suspended

solids (TSS) concentration of  $1\text{--}2 \text{ g L}^{-1}$  to avoid light hindrance, by controlling sludge retention time (SRT) (Arashiro et al., 2017) and the synthetic feed; c) avoidance of the presence of nitrate in the anaerobic stage by suppressing the growth of nitrifying organisms in the EBPR-PAS system by applying a minimum net aerobic SRT of 3 days (Brdjanovic et al., 1998) and through the addition of a nitrification inhibitor; d) avoidance of P-limiting conditions for PAOs and microalgae by taking into account the maximum poly-P storage of PAOs ( $f_{p,vss \text{ PAOs}}$ ) (38% of volatile suspended solids (VSS); Wentzel et al., 1990) and the minimum requirements to cover the microalgal growth requirements ( $f_{p,vss \text{ algae}}$ ) (1.3% VSS; Mara, 2004); e) supplying enough ammonium-N ( $\text{NH}_4\text{-N}$ ) in the feed for PAOs (10% VSS; Henze et al. 2008) and microalgae (9.2% VSS; Mara, 2004); f) adjusting the inorganic carbon concentration in the feed taking into account the  $\text{CO}_2$  generation of PAOs so that microalgae should be the only source of oxygen for PAOs when implementing the illuminated stage; and g) light requirement was estimated taking into account light penetration/attenuation as a function of the TSS concentration using the Lambert-Beer equation (Swinehart, 1962) (Appendix B).

Fig. 1 shows the summary results of the model. For balanced PAOs-microalgae symbiosis, the model suggested the composition of the synthetic wastewater should contain  $100 \text{ mg L}^{-1}$  of COD,  $12 \text{ mg L}^{-1}$  of  $\text{PO}_4\text{-P}$ ,  $88 \text{ mg L}^{-1}$  of  $\text{HCO}_3^-$ , and  $10 \text{ mg L}^{-1}$  of  $\text{NH}_4\text{-N}$  (Fig. 1-a,b). Under these conditions, the overall VSS and TSS concentrations were estimated at  $1.08 \text{ g L}^{-1}$  and  $1.6 \text{ g L}^{-1}$  (Fig. 1-c), respectively, which were within the limits specified in the assumptions. Moreover, the oxygen produced by microalgae would be double the PAOs requirements (Fig. 1-b). Based on the prediction of the model, these concentrations were applied to the start-up phase with only minor modifications: the inorganic carbon was  $200 \text{ mg HCO}_3^- \text{ L}^{-1}$  instead of  $88 \text{ mg HCO}_3^- \text{ L}^{-1}$  (Fig. 1-b), which supplied the total inorganic carbon required, not assuming that PAOs would retrieve the theoretically calculated  $112 \text{ mg HCO}_3^- \text{ L}^{-1}$  (Fig. 1-b) as  $\text{CO}_2$  anaerobically and aerobically according to Smolders et al. (1994a,b). The model estimated an incident light intensity of  $145 \mu\text{mol m}^{-2} \text{sec}^{-1}$  (Table A.3, Appendix A) for the photosynthesis process. However, a light intensity of  $350 \mu\text{mol m}^{-2} \text{sec}^{-1}$  was used in the start-up phase to avoid light limitation for microalgal growth.

### 2.2. Reactor configuration and enrichment of the EBPR-PAS system

Two cylindrical double-jacketed glass reactors, each with an internal diameter of 12.5 cm and an active volume of 2.5 L, were used in the study. Reactor One (R1; Fig. 2) was the main reactor and used for the enrichment and development of the PAOs-microalgae consortia to test the synergetic effect of microalgae and PAOs to perform EBPR (referred to as an EBPR-PAS system). Reactor Two (R2), the study control, was operated as a conventional EBPR (without microalgae and light) (referred to as an EBPR system). R1 was inoculated with 600 ml of activated sludge from a wastewater treatment plant (WWTP) (Harnaschpolder, Den Horn, The Netherlands) with a TSS concentration of  $6 \text{ g L}^{-1}$ . The activated sludge was mixed with 600 ml of five species of microalgae/cyanobacteria (120 ml each; *Scenedesmus quadricauda*, *Anabaena variabilis*, *Chlorella sp.*, *Chlorococcus sp.*, *Spirulina sp.*) with an average concentration of  $1 \text{ g TSS L}^{-1}$ , similar to those used by van der Steen et al. (2015). This led to a total initial TSS concentration of  $1.75 \text{ g L}^{-1}$  in R1. R2 was inoculated with an enriched culture of PAOs from an EBPR reactor (Welles et al., 2017). Due to operational challenges with R1, which showed poor EBPR activities in the start-up phase, 25 to 30 ml of enhanced PAOs culture from R2 was seeded on daily basis to the microalgae biomass in R1 from day 25 to 36 and day 41.

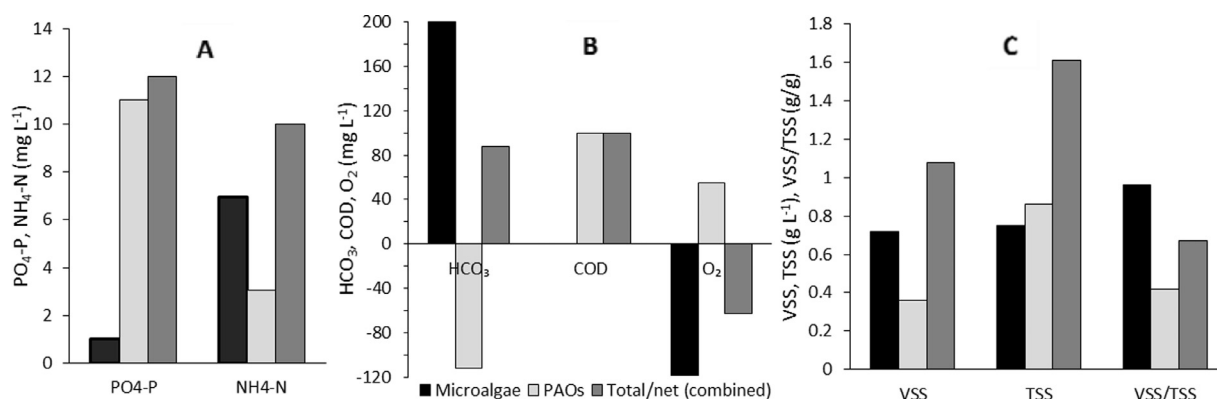


Fig. 1. Model results for: a) influent concentrations of PO<sub>4</sub>-P and NH<sub>4</sub>-N; b) concentrations of HCO<sub>3</sub>, COD, and O<sub>2</sub> (positive values mean consumption/uptake, and negative values mean production/release); and c) the relevant generated biomass (VSS, TSS, VSS/TSS) for microalgae, PAOs and combination.

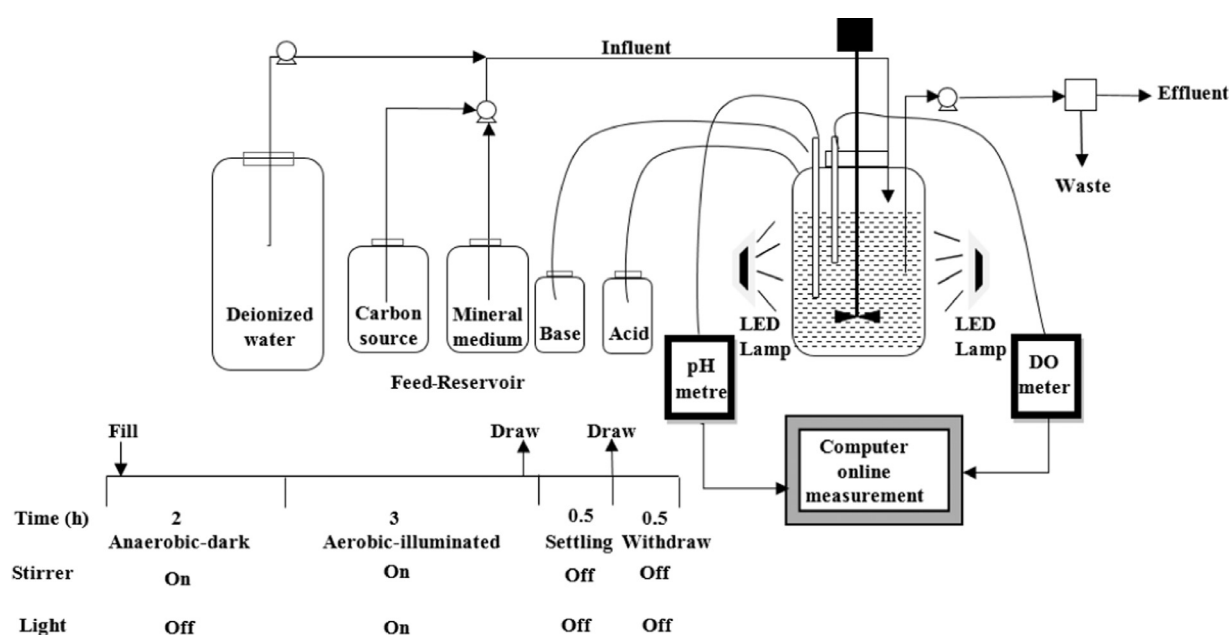


Fig. 2. Main reactor set-up (R1)

The EBPR-PAS system (R1) was operated under alternating anaerobic-aerobic EBPR conditions, with dark conditions during the anaerobic stage and illuminated conditions during the aerobic stage, to enhance the growth of microalgae. To achieve this, R1 was run as an SBR with four cycles of 6 h per day, comprising a 2 h dark/anaerobic stage, a 3 h illuminated/aerobic stage, a 0.5 h settling stage, and a 0.5 h effluent withdrawal stage (Fig. 2). An ADI controller and BioXpert software (Applikon, Delft, The Netherlands) were used to operate the SBR and for data acquisition. Mixing took place in the dark/anaerobic and illuminated/aerobic stages at 500 rpm (van Loosdrecht et al., 2016). The temperature was maintained at 20 ± 1°C throughout all stages by a LAUDA system (Lauda-Königshofen, Germany). The pH was maintained at 7.5 ± 0.1 to favor PAOs over glycogen-accumulating organisms (GAO; Lopez-Vazquez et al., 2009), through the automatic dosing of either 0.4 M HCl or 0.4 M NaOH. For illumination, eight light-emitting-diode (LED) lamps (40W, Phillips, The Netherlands) were used, with four of each located at opposite sides of the reactor. During each cycle, from min 5 to min 10 of the anaerobic stage, synthetic wastewater was pumped from the influent feeding tank to R1 using a peri-

static pump, while a second peristaltic pump, positioned in R1, served two purposes: to withdraw 105 ml of the mixed liquor for the last 5 mins of the aerobic stage, thereby controlling the SRT to 6 days, and to discharge the effluent during the withdrawal stage (Fig. 2). During the effluent withdrawal stage, half of the working volume was removed, so as to attain an hydraulic retention time (HRT) of 12 h. During the start-up phase (P1), an air compressor, controlled by an on-off valve, supplied the oxygen to the reactor during the aerobic period at a point not exceeding 20% of saturation (around 1.8 mg L<sup>-1</sup>). The air compressor was not used when the system was solely dependent on the microalgae oxygen in the phases following the start-up phase. Nitrogen gas (N<sub>2</sub>) was sparged into the reactor during the first 25 mins of the anaerobic stage to generate anaerobic conditions.

R2 contained the same medium and had the same operational conditions as in R1 (SRT: 6 days, HRT: 12 h). However, oxygen was supplied to R2 during all the cycles of the aerobic stages, whereas in R1, because of the reliance on microalgae to provide oxygen, external aeration was supplied only in the start-up phase (P1) when the dissolved oxygen (DO) saturation dropped below 20%. In addi-

**Table 1**  
Operational conditions of the main reactor (R1) during the study period of 100 days.

Phase	SRT (days)	HRT (hrs)	External aeration	Light intensity $\mu\text{mol m}^{-2} \text{sec}^{-1}$	COD:HCO <sub>3</sub> :NH <sub>4</sub> -N	Seeding of PAOs from R2	Operational days
P1	6	12	+/-	350	10:20:1	+++	40
P2	6	12	-	350	10:10:4	+/-	40
P3	6	12	-	350, 262.5, 175, 87.5	10:10:4	-	20

(+) with external aeration or PAOs seeding (-) without external aeration or PAOs seeding

tion, R2 was not exposed to alternating dark and illumination conditions as was the case with R1.

### 2.3. Experimental phases and synthetic medium

Table 1 shows the operating conditions for the EBPR-PAS system, which were determined based on the outcomes of the model-based design. It comprised three experimental phases, with a total duration of 100 days. In phase 1 (P1), the EBPR-PAS system was loaded with synthetic wastewater [COD:100 mg L<sup>-1</sup>; P:12 mg L<sup>-1</sup>; COD:HCO<sub>3</sub>:NH<sub>4</sub>-N of 10:20:1 mg:mg:mg]. After ensuring that the microalgae were growing well enough to produce sufficient oxygen (DO saturation level > 20%), the external aeration supply was gradually reduced over 11 days until the EBPR-PAS system operated without external aeration. In phase 2 (P2), in order to optimize the nutrients and avoid limiting growth conditions for both organisms, the NH<sub>4</sub>-N concentration was increased by a factor of four and the inorganic carbon reduced by half (COD:HCO<sub>3</sub>:NH<sub>4</sub>-N of 10:10:4 mg:mg:mg), and the system was allowed to stabilize. When no significant changes in the effluent parameters were observed (for at least 3\*SRT= 18 days), the system was assumed to have reached pseudo-steady-state conditions. In phase 3 (P3), the short-term effects of different incident light intensities (350, 262.5, 175, and 87.5  $\mu\text{mol m}^{-2} \text{sec}^{-1}$ ), each lasting three days, were investigated on the last day for each light intensity. These intensities were within the range reported by EUMETSAT (2020) in Northern European conditions. This phase aimed to study the effect of light intensity on DO generation, and evaluate the culture response to light fluctuations and, therefore, the performance of the EBPR-PAS system.

The influent wastewater comprised a carbon source, a mineral medium, and deionized water, each contained in separate containers (Fig. 2). The carbon source consisted of 3:1 acetate: propionate. This COD ratio favors the growth of PAOs over GAO (Lopez-Vazquez et al., 2009). The carbon source and mineral medium were autoclaved for one hour at 115°C before use. The final composition of wastewater in the influent consisted of: 160 mg L<sup>-1</sup> of NaAc.3H<sub>2</sub>O (2.36 C-mmol L<sup>-1</sup>, 75 mg COD L<sup>-1</sup>), 0.0167 ml of C<sub>3</sub>H<sub>6</sub>O<sub>2</sub> (0.68 C-mmol L<sup>-1</sup>, 25 mg COD L<sup>-1</sup>), 38 mg L<sup>-1</sup> of NH<sub>4</sub>Cl (0.715 N-mmol L<sup>-1</sup>, 10 mg N L<sup>-1</sup>) (increased to 152 mg L<sup>-1</sup> (2.86 N-mmol L<sup>-1</sup>, 40 mg N L<sup>-1</sup>) in P2 and P3), 48 mg L<sup>-1</sup> of NaH<sub>2</sub>PO<sub>4</sub> (0.4 P-mmol L<sup>-1</sup>, 12 mg P L<sup>-1</sup>), 280 mg L<sup>-1</sup> of NaHCO<sub>3</sub> (3.34 C-mmol L<sup>-1</sup>, 200 mg HCO<sub>3</sub> L<sup>-1</sup>) (reduced to 140 mg L<sup>-1</sup> (1.67 C-mmol L<sup>-1</sup>, 100 mg HCO<sub>3</sub> L<sup>-1</sup>) in P2 and P3), 75 mg L<sup>-1</sup> of MgSO<sub>4</sub>.7H<sub>2</sub>O, 36 mg L<sup>-1</sup> of CaCl<sub>2</sub>.2H<sub>2</sub>O, 16.0 mg L<sup>-1</sup> of KCl, 3.4 mg L<sup>-1</sup> of FeSO<sub>4</sub>.7H<sub>2</sub>O, 10 mg L<sup>-1</sup> of EDTA.Na<sub>2</sub>, 2 mg L<sup>-1</sup> of allyl-N-thiourea (ATU) to inhibit nitrification, 1 mg L<sup>-1</sup> of yeast extract, and trace elements as described in Becker (1994) for microalgae growth. The trace elements receipt also attained PAOs requirements as described by Smolders et al. (1994a,b). Influent concentrations were diluted after mixing with the half reactor volume remaining from the previous cycle.

### 2.4. Analysis

Acetate and propionate were measured using Varian 430-GC Gas Chromatography (Varian BV, The Netherlands) equipped with

a split injector (200°C), a WCOT Fused Silica column (105°C) and coupled to a FID detector (300°C). Helium gas was used as the carrier gas and 50 mL of butyric acid as the internal standard. Ammonium was measured using spectrophotometric methods as described in NEN 6472 (1983). Phosphate was measured using the ascorbic acid spectrophotometric method as described in APHA (2005). Samples that were not analyzed immediately were preserved at 4°C for NH<sub>4</sub>-N and PO<sub>4</sub>-P measurements and -20°C for VFA measurements for a maximum of one week before analysis. Total inorganic carbon (TIC) was measured using a TOC-L analyzer equipped with an ASI-L autosampler (Shimadzu, Kyoto, Japan). Total suspended solids and VSS were measured using gravimetric techniques (APHA, 2005). Light intensity was measured using a light meter Li-250 (Li-COR, United States). Chlorophyll-*a* was measured using the ethanol extraction Spectrophotometric method, described in the Dutch standard method (NEN 6520, 1982). An Avantium Crystalline PV (Crystalline analyzer) was used to investigate particle size distribution of the flocs. For the identification of microalgae/cyanobacteria species based on morphology, an advanced optical microscope Olympus BX53 (Shinjuku, Tokyo, Japan) was used. To enhance the visualization of the mixed culture cells, DAPI staining was applied to record prokaryotic/bacteria and eukaryotic/microalgae DNA through fluorescence (Nielsen and Daims, 2009). The pictures were then captured with an Olympus BX51 (Shinjuku, Tokyo, Japan).

### 2.5. Calculations

#### 2.5.1. Sludge volume index

To calculate the sludge volume index (SVI) (Eq. 1), the mixed culture was poured into a 2 L capacity vertical cylinder and allowed to settle. The settled sludge volume was measured after 30 mins, and the TSS concentration of the mixed culture was measured gravimetrically (APHA, 2005).

$$SVI \text{ (ml g}^{-1}\text{)} = \frac{\text{Settled sludge volume (ml L}^{-1}\text{)} \times 1000}{\text{Suspended solids (mg L}^{-1}\text{)}} \quad (1)$$

#### 2.5.2. Kinetic and stoichiometric parameters

The kinetic profiles of NH<sub>4</sub>-N, PO<sub>4</sub>-P, VFAs, TIC, and DO in P1-P3 were monitored to assess the performance of the EBPR-PAS system and were also used as metrics to adjust the medium composition in P2.

The maximum P release rate (in mg PO<sub>4</sub>-P L<sup>-1</sup> h<sup>-1</sup>) was calculated from the slope of the graph by adjusting the linear regression line to the experimental concentrations determined along the highest P release period (start of dark/anaerobic stage). Phosphorus release (in mg PO<sub>4</sub>-P L<sup>-1</sup>) was calculated as the difference between P concentrations at the start and end of the dark-anaerobic stage (Eq. 2).

$$P_{\text{release}} = P_{\text{end of anaerobic}} - P_{\text{start of anaerobic}} \quad (2)$$

The maximum P uptake rate (mg PO<sub>4</sub>-P L<sup>-1</sup> h<sup>-1</sup>) was calculated from the slope of the graph by adjusting the linear regression line to the experimental concentrations determined during the highest P uptake period (start of illuminated/aerobic stage). Total P uptake

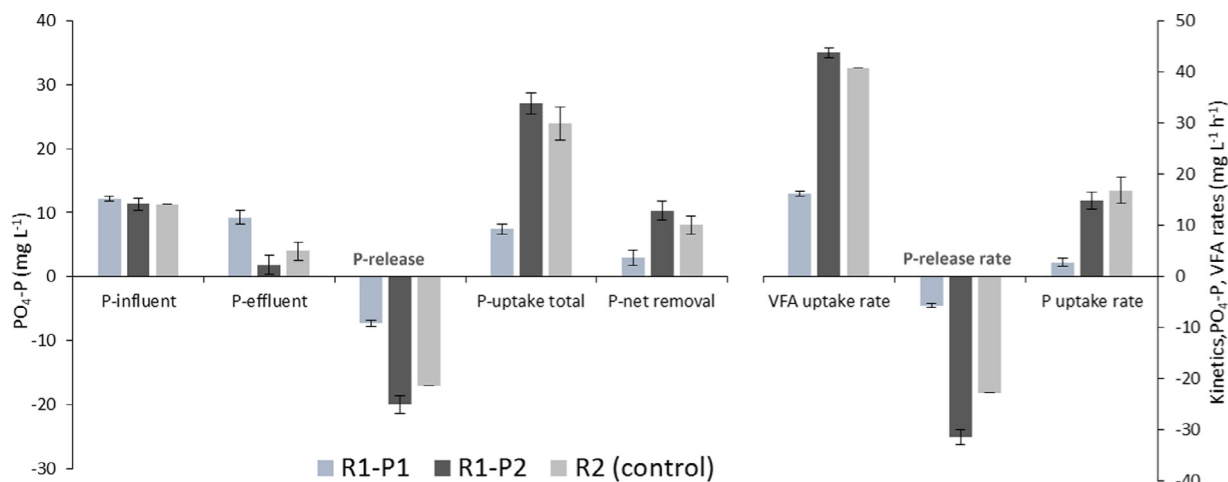


Fig. 3. Phosphorus and VFA parameters for the EBPR-PAS system (R1) during P1 and P2, and the control reactor (conventional EBPR system, R2)

(in mg PO<sub>4</sub>-P L<sup>-1</sup>) was calculated as the difference between P concentrations at the start and end of the illuminated/aerobic stage (Eq. 3).

$$P_{\text{uptake total}} = P_{\text{start of aerobic}} - P_{\text{end of aerobic}} \quad (3)$$

The net P removal (in mg PO<sub>4</sub>-P L<sup>-1</sup>) was calculated as the difference between P concentrations of the influent and at the end of a 6 h cycle (Eq. 4).

$$P_{\text{net-removal}} = P_{\text{influent}} - P_{\text{effluent}} \quad (4)$$

The maximum VFA uptake rate (in mg COD L<sup>-1</sup> h<sup>-1</sup>) was calculated from the slope of the graph by adjusting the linear regression line to the experimental concentrations determined along the highest VFA uptake period (start of dark/anaerobic stage). VFA consumed (in mg COD L<sup>-1</sup>) was calculated as the difference between COD concentrations at the start and end of the dark/anaerobic stage (Eq. 5).

$$VFA_{\text{consumed}} = VFA_{\text{start of anaerobic}} - VFA_{\text{end of anaerobic}} \quad (5)$$

Phosphorus release/VFA consumed was calculated and presented as P-mmol/C-mmol. The NH<sub>4</sub>-N uptake rate (in mg NH<sub>4</sub>-N L<sup>-1</sup> h<sup>-1</sup>) was calculated from the slope of the graph by adjusting the linear regression line to the experimental concentrations determined along the different periods of the illuminated/aerobic stage. Statistical analysis was performed using the t-test (two-tailed) using Excel. The standard error (SE) was calculated using Eq. (6):

$$SE = STDEV/\sqrt{N} \text{ (where N is the number of samples)}. \quad (6)$$

### 3. Results and discussion

#### 3.1. First experimental phase (COD:HCO<sub>3</sub>:NH<sub>4</sub>-N of 10:20:1)

Phase 1 (P1) was the starting point of the EBPR-PAS cultivation system based on the steady-state model prediction (COD:HCO<sub>3</sub>:NH<sub>4</sub>-N: 10:20:1). The EBPR-PAS system (R1) displayed excellent algal/photosynthesis activities as measured by the utilization of inorganic carbon and the production of oxygen, which occasionally exceeded 300% of the saturated DO. However, R1 demonstrated poor P release and uptake (Fig. 3). The P release and total P uptake for R1 in P1 were  $7.3 \pm 0.48$  mg L<sup>-1</sup> (SE= 0.24, n= 4) and  $7.2 \pm 2.8$  mg L<sup>-1</sup> (SE= 1.05, n= 7; Fig. 3), respectively. Overall, R1 had a final effluent P concentration of  $9.45 \pm 1.05$  mg L<sup>-1</sup> (SE= 0.25, n= 9), with a net P removal of only  $2.75 \pm 1.05$  mg L<sup>-1</sup> (SE= 0.25, n= 9; Fig. 3). In contrast, the conventional EBPR system, R2 (control), demonstrated good P release and P uptake (Fig. 3). The

P release rate during the anaerobic stage for R2 ( $23$  mg L<sup>-1</sup> h<sup>-1</sup>) was four times higher than R1 ( $5.7$  mg L<sup>-1</sup> h<sup>-1</sup>; Fig. 3). The maximum P uptake rate during the aerobic period for R2 ( $16.87$  mg L<sup>-1</sup> h<sup>-1</sup>) was almost six times higher than in R1 ( $2.76$  mg L<sup>-1</sup> h<sup>-1</sup>; Fig. 3). Moreover, the anaerobic consumption rate of VFA by PAOs for R2 ( $40.2$  mg L<sup>-1</sup> h<sup>-1</sup>) was 2.5 times higher than R1 ( $16$  mg L<sup>-1</sup> h<sup>-1</sup>; Fig. 3). Overall, the average P release and total P uptake for R2 were  $17.1 \pm 1.3$  mg L<sup>-1</sup> and  $24 \pm 2.5$  mg L<sup>-1</sup> (SE= 1.04, n= 6; Fig. 3), respectively. This make R2 had an effluent P concentration of  $4.0 \pm 1.4$  mg L<sup>-1</sup> (SE= 0.41, n= 12), with a net P removal of  $8.01 \pm 1.38$  mg L<sup>-1</sup> (SE= 0.4, n= 12; Fig. 3).

To improve R1 performance, 25 to 30 ml of enhanced PAOs culture (VSS=  $0.4 \pm 0.03$  g L<sup>-1</sup>, TSS=  $0.7 \pm 0.06$  g L<sup>-1</sup>) from R2 was seeded regularly to the microalgae biomass in R1 from day 25 to 36. Despite this addition, R1 did not demonstrate any capacity for P removal during P1, although both R1 & R2 were supplied with the same medium and operated under the same conditions. The poor growth of PAOs culture in R2 may have been due to different stresses in the cultivation system (e.g. O<sub>2</sub> saturation, nutrient stress (competition for NH<sub>4</sub>-N), micro-algal concentration, sludge age). Therefore, the interplay between PAOs and microalgae was not balanced, with microalgae dominating P1.

To investigate the cause of the poor P removal in R1, kinetic studies were performed for R1 (on day 24) and R2 (on day 33), and compared to each other (Fig. 4a-c). The results showed that only  $20$  mg L<sup>-1</sup> of COD was consumed during the anaerobic stage, and more than half the influent COD ( $30$  mg L<sup>-1</sup>; Fig. 4a) escaped into the aerobic stage for R1. On the other hand, the influent COD was fully consumed and stored by PAOs in the anaerobic stage for R2 (Fig. 4a), which was an indication of good EBPR activity. The P profile in Fig. 4b shows both P release and P uptake were very low in R1 compared to R2: the maximum P release rate during the anaerobic stage for R2 ( $23$  mg L<sup>-1</sup> h<sup>-1</sup>) was eight times higher than R1 ( $3$  mg L<sup>-1</sup> h<sup>-1</sup>; Fig. 4b). The maximum P uptake rate during the aerobic period for R2 ( $16.87$  mg L<sup>-1</sup> h<sup>-1</sup>) was almost six times higher than in R1 ( $2.72$  mg L<sup>-1</sup> h<sup>-1</sup>; Fig. 4b). The NH<sub>4</sub>-N profile in Fig. 4c shows that NH<sub>4</sub>-N uptake in R1 started from the beginning of the aerobic stage, with a rate of  $3.37$  mg NH<sub>4</sub>-N L<sup>-1</sup> h<sup>-1</sup>, and was almost fully consumed within the first 45 mins. In R2, there was a 30 minute lag in the aerobic stage before PAOs started to uptake NH<sub>4</sub>, and then uptake occurred at  $0.44$  mg-NH<sub>4</sub>-N L<sup>-1</sup> h<sup>-1</sup>, a lower rate than observed in R1 (Fig. 4c). As a result of the higher NH<sub>4</sub>-N uptake in R1, PAOs growth in this system was likely inhibited by a shortage of N, although the total demand of NH<sub>4</sub>-N by PAOs was very low according to R2 as shown in Fig. 4c. Thus,

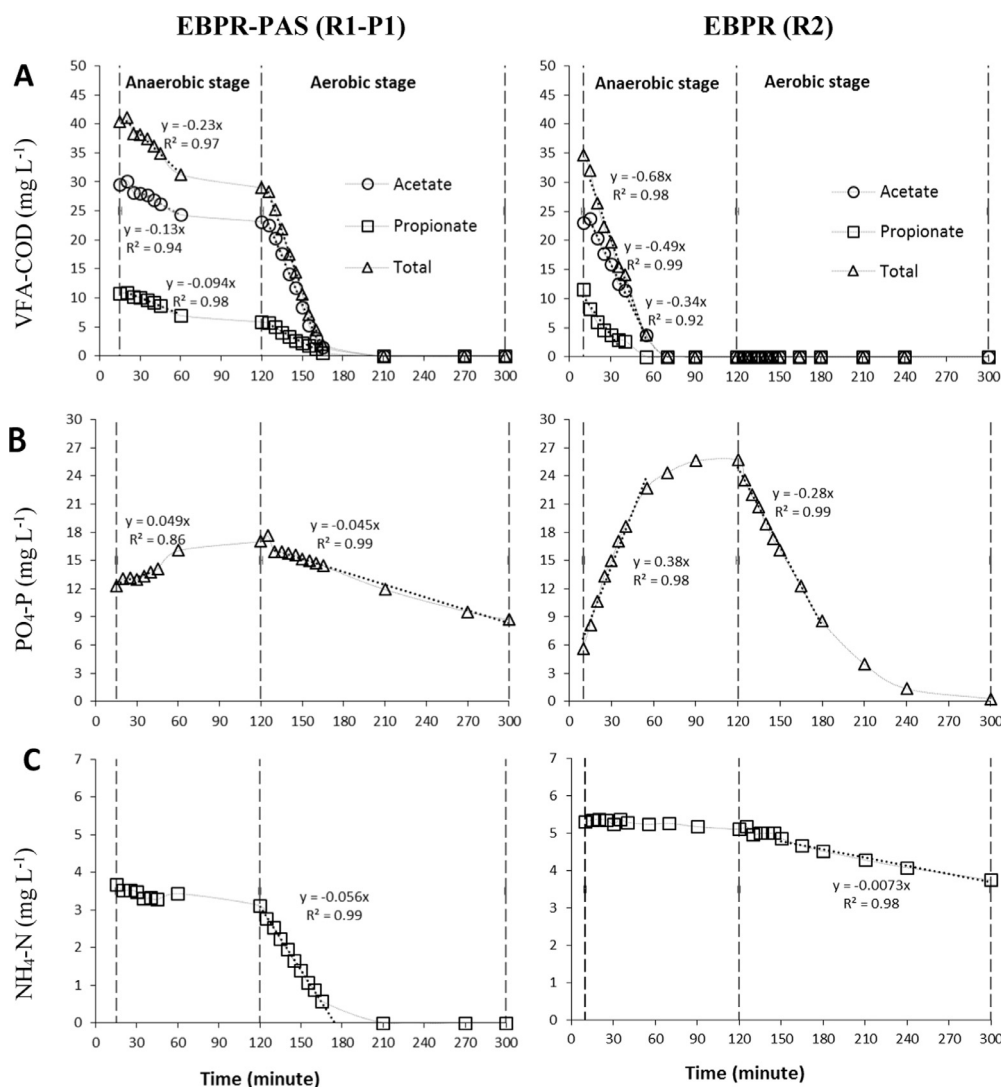


Fig. 4. Kinetic studies for R1 during P1 on day 24 of operation (left) and R2 on day 33 of operation (right); A) VFAs profile; B) phosphate profile; C) ammonium-N profile.

ammonium was likely taken up by microalgae and potentially by other organisms rather than PAOs in R1. Moreover, the loss of NH<sub>4</sub> by nitrification was not expected due to the addition of the nitrification inhibitor, ATU.

Therefore, the NH<sub>4</sub>-N concentration in the influent of R1 was increased from 10 mg L<sup>-1</sup> to 40 mg L<sup>-1</sup> to meet PAOs requirements. Also, the inorganic carbon concentration in the influent was decreased from 200 mg HCO<sub>3</sub> L<sup>-1</sup> to 100 mg HCO<sub>3</sub> L<sup>-1</sup>, to limit the excess NH<sub>4</sub>-N uptake by microalgae. Despite this, the new value of the inorganic carbon met the model requirement (88 mg HCO<sub>3</sub> L<sup>-1</sup>; Fig. 1-b), because the initial concentration of inorganic carbon that had been added in P1 did not consider the inorganic carbon produced by PAOs (Section 2.1).

### 3.2. Second experimental phase (COD:HCO<sub>3</sub>:NH<sub>4</sub>-N of 10:10:4)

Effective conditions were established by adjusting the nutrient composition (COD, HCO<sub>3</sub>, and NH<sub>4</sub>-N) to a ratio of (10:10:4) according to the results of the kinetic studies in P1. Both P release and P uptake within R1 improved significantly ( $P < 0.0001$ ) during P2, and the results were comparable to the control reactor (R2; Fig. 3). The average P release and total P uptake by R1 were  $20 \pm 1.43$  mg L<sup>-1</sup> mg L<sup>-1</sup> (SE= 0.5, n= 8) and  $27.8 \pm 1.8$  mg L<sup>-1</sup> (SE= 0.48, n= 14; Fig. 3), respectively. The average P concentration in

the final effluent for R2 was  $1.87 \pm 1.45$  mg L<sup>-1</sup> (SE= 0.25, n= 34), with a net removal of  $10.33 \pm 1.45$  mg P L<sup>-1</sup> (SE= 0.25, n= 34; Fig. 3).

The total COD was fully consumed during the first hour of the anaerobic stage at a rate of 40 mg L<sup>-1</sup> h<sup>-1</sup> (Fig. 5a), a rate that was similar to previous measurements for R2 (Fig. 4a), and almost three times higher than that achieved in P1 for R1 (Fig. 4a, Fig. 5a). Correspondingly, the P release rate for R1 increased three-fold from 8.4 mg L<sup>-1</sup> h<sup>-1</sup> in P1 to 28.2 mg L<sup>-1</sup> h<sup>-1</sup> in P2 (Fig. 5b), and P uptake rate for R1 increased six-fold from 2.82 mg L<sup>-1</sup> h<sup>-1</sup> in P1 to 16.8 mg L<sup>-1</sup> h<sup>-1</sup> in P2 (Fig. 5b), which was similar to R2 (Fig. 4b). Fig. 5c shows there was a lot of ammonium left in the effluent in P2, and the uptake rate was reduced from 3.84 mg L<sup>-1</sup> h<sup>-1</sup> in P1 to nearly half in P2 (2.3 mg L<sup>-1</sup> h<sup>-1</sup>) (Fig. 5c). This decrease was possibly due to the reduction in microalgal biomass as a result of reducing influent inorganic carbon. However, the NH<sub>4</sub>-N uptake rate of R1 in P2 was still higher than R2 (Fig. 4c), because microalgae and PAOs will co-contribute to the uptake rate of NH<sub>4</sub>-N in R1. The total NH<sub>4</sub>-N uptake in P2 was 4.9 mg L<sup>-1</sup> (Fig. 5c; 9.8 mg L<sup>-1</sup> as an influent concentration before dilution). This concentration was similar to the NH<sub>4</sub>-N supplied in P1. Therefore, inorganic carbon reduction was a key adjustment to limit microalgal growth and cultivate a successful symbiotic relationship between microalgae and PAOs.

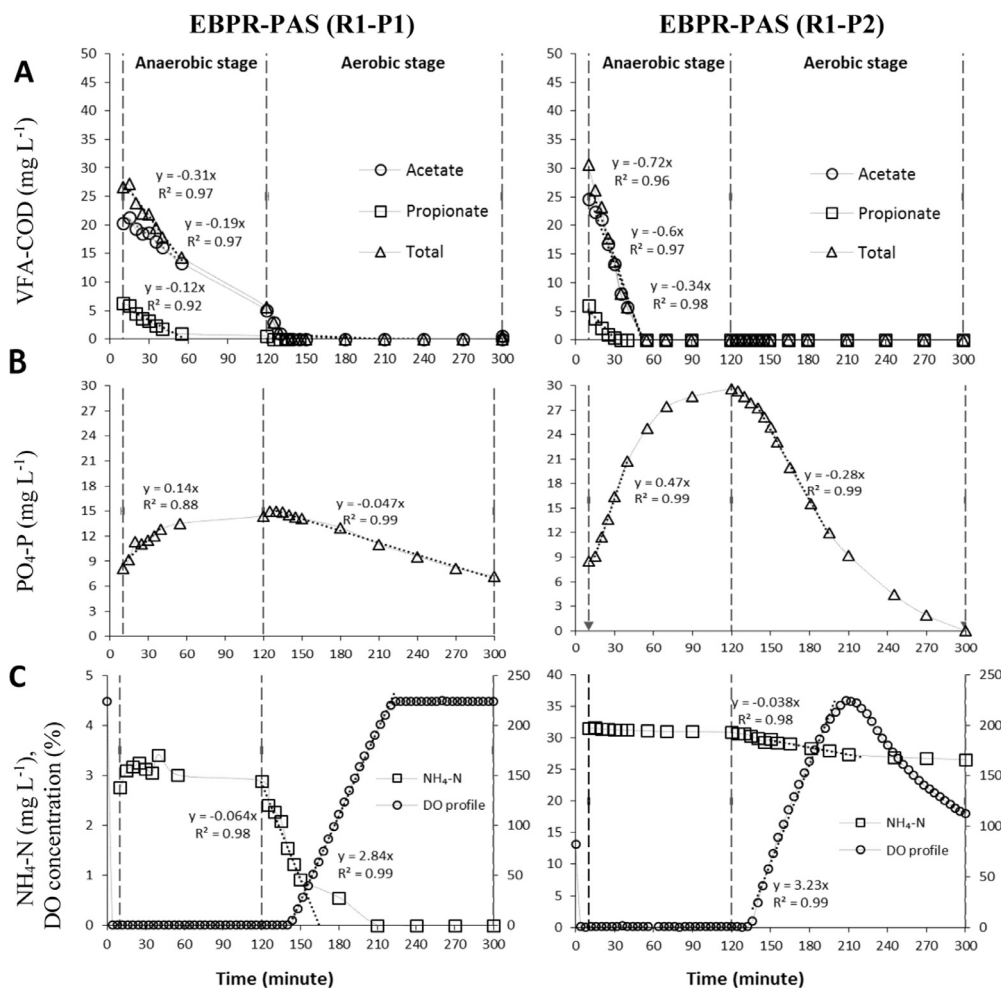


**Fig. 5.** Kinetic studies for R1 during P1 on day 26 of operation (left) and P2 on day 64 of operation (right); a) VFAs profile; b) phosphate profile; c) ammonium profile combined with DO profile.

In P2, there was a reduction in the DO concentration in the middle of the aerobic stage, which coincided with the depletion of inorganic carbon (Fig. 6) as microalgae were no longer able to perform photosynthesis in the absence of inorganic carbon. This indicates that limiting the microalgae growth by controlling the inorganic carbon was a successful measure. The medium (COD:HCO<sub>3</sub>:NH<sub>4</sub>-N) in P2 was supplied at a ratio of 10:10:4, but the actual consumption ratio was 10:10:1, which was similar to that predicted by the model when considering that PAOs contributed part of HCO<sub>3</sub> as CO<sub>2</sub> (ratio of 100:88:10; Fig. 1-a,b). PAOs managed to contribute 8.03 mg CO<sub>2</sub> L<sup>-1</sup> (11.13 mg L<sup>-1</sup> as HCO<sub>3</sub>) anaerobically (Fig. 6), which was almost similar to the model estimation of 11 mg CO<sub>2</sub> L<sup>-1</sup> (Table A3, Appendix A). The initial approach adopted in P1 was to avoid limiting conditions for microalgae growth, and therefore inorganic carbon was supplied in abundance in P1 (not considering the share provided by PAOs). This measure potentially generated excess microalgal biomass in P1 which outcompeted PAOs for NH<sub>4</sub>-N.

### 3.3. EBPR-PAS system performance and characteristics

At steady-state, an enmeshed mixed culture of PAOs and microalgae was obtained from R1 in P2 (Appendix C). The average TSS concentration was  $1108.06 \pm 154.9$  mg L<sup>-1</sup> (SE = 41.4, n=17), with an average VSS of  $839.18 \pm 137$  mg L<sup>-1</sup> (SE = 33.24, n=17) and a VSS/TSS ratio of  $0.75 \pm 0.027$  (SE = 0.007, n=17; Fig. 7), which was close to the model predictions (Fig. 1-c). The lower VSS/TSS ratio in P2 (0.75) than in P1 (0.99; Fig. 7) was an indi-

cator of improving EBPR activities in R1 during P2. PAOs generate inactive biomass/inert suspended solids (ISS) from the stored poly-P and associated counter ions (Mg<sup>+2</sup>, K<sup>+1</sup>, and Ca<sup>+2</sup>), and therefore have a low VSS/TSS ratio (Ekama and Wentzel, 2004), while microalgae generate less ISS. Consequently, the VSS/TSS ratio is lower for a conventional EBPR system (R2) than an EBPR-PAS system (R1). This was apparent in the current study and that of Carvalho et al. (2018), as respective VSS/TSS ratios of 0.75 (Fig. 7) and 0.68-0.8 were recorded for EBPR-PAS systems. A VSS/TSS ratio of 0.58 was achieved in R2 of the current study (Fig. 7) and by Welles et al. (2015) for a conventional EBPR system.

Phosphorus release/VFA consumed was  $0.58 \pm 0.04$  P-mmol/C-mmol during P2, which was similar to R2 (Fig. 7). This was also an indication of good EBPR activity according to the results of Welles et al. (2017) and Saad et al. (2016), who reported values of between 0.4 and 0.8 P-mmol/C-mmol for PAOs in conventional EBPR systems.

The total NH<sub>4</sub>-N consumption by biomass (microalgae + PAOs) was  $9.3 \pm 0.74$  mg L<sup>-1</sup> (SE = 0.25, n = 11; Fig. 7) during P2. This value was approximately equal to that predicted by the model (10 mg L<sup>-1</sup>), in which PAOs and microalgae account for NH<sub>4</sub>-N uptake of 3.04 and 6.96 mg L<sup>-1</sup>, respectively (Fig. 1-a).

During P2, COD consumed/average P net removal for R1 (100/10.4) was lower than R2 (100/8). This indicates that the EBPR-PAS system required less organic carbon than the conventional EBPR system. On days 62, 63, 64, 68, 69, and 76, the



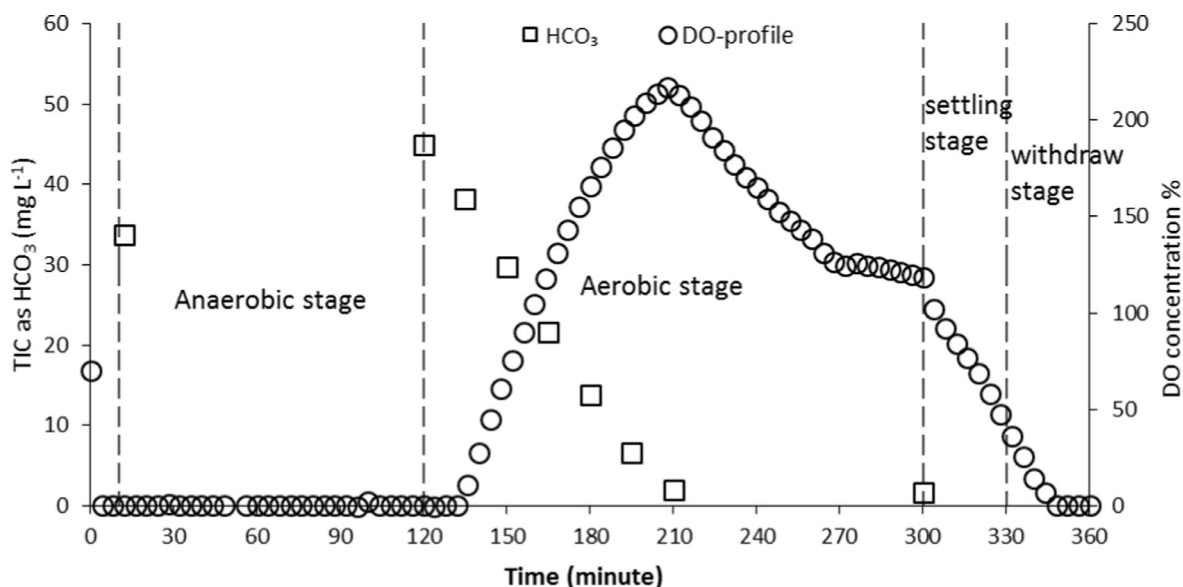


Fig. 6. Kinetic study of total inorganic carbon (as  $\text{HCO}_3^-$ ) combined with the DO online profile for R1 in P2 on day 49 of operation.

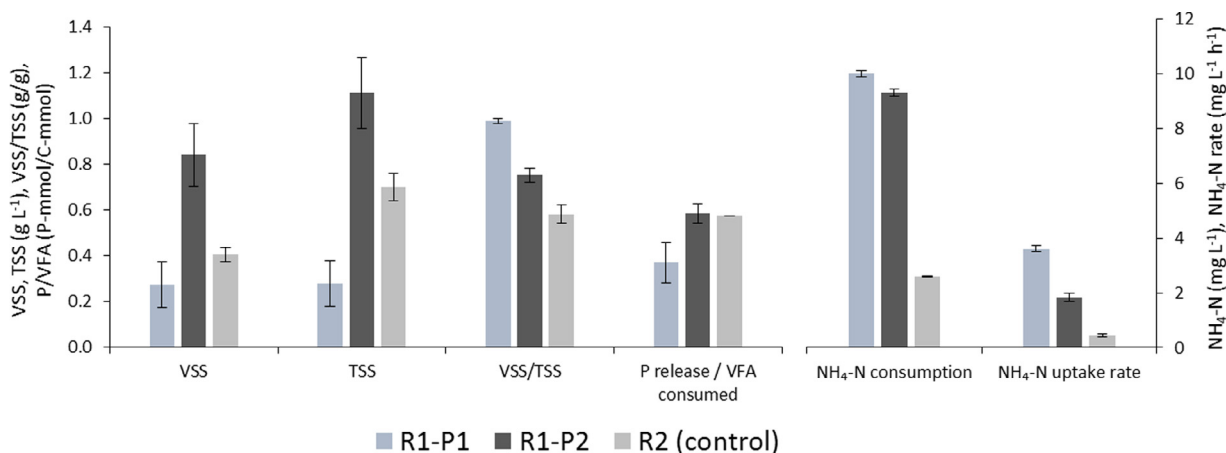


Fig. 7. VSS, TSS, VSS/TSS, P-release/VFA consumed, total  $\text{NH}_4\text{-N}$  consumption, and  $\text{NH}_4\text{-N}$  uptake rate for the EBPR-PAS system (R1) during P1 and P2, and the control reactor (conventional EBPR system, R2)

system was capable of complete  $\text{PO}_4$  removal, without the supply of any external aeration (Appendix D, Fig. D.1, Fig. D.2), and with a low COD/P net removal ratio of 100/12 in which PAOs and microalgae account for P removal of 11 and 1  $\text{mg L}^{-1}$ , respectively, according to the model (Fig. 1-a). The COD/P net removal of 100/12 was lower than that achieved in the literature for best performing conventional EBPR systems. For example, Carvalho et al. (2014a) achieved a COD consumed/P net removal of 200/20, with an influent P concentration of 20  $\text{mg L}^{-1}$  for conventional EBPR reactor. Carvalho et al. (2018) also reported very low COD consumed/P net removal (200/34) for an EBPR-PAS system, with an influent P concentration of 60  $\text{mg L}^{-1}$ . The main reason for this low COD/P net removal for an EBPR-PAS system was that microalgae participated in P removal (1.3 % of microalgae biomass), without requiring COD (with inorganic carbon as the carbon source). In contrast, the EBPR-PAS system of the current study (R1) and Carvalho et al. (2018) had a lower capacity to remove phosphate per g biomass (P/VSS) than the conventional EBPR system (R2). This because PAOs can uptake P to a maximum of 38% of their biomass (Wentzel et al., 1990), while microalgae typically can only uptake P to 1.3% of their biomass (Mara, 2004). However, there are some types of microalgae/cyanobacteria capable of

acting as PAOs that can significantly contribute to poly-P storage. For example, Ji et al. (2020b) found that the cyanobacteria *Pantalaninema spp.* were the major phosphorus-accumulating organisms in microalgal-bacterial granular sludge, although the P content of this cyanobacteria was far less than 38% of VSS. Therefore, for similar amounts of phosphate removal, an EBPR-PAS system requires less organic carbon and generates higher biomass than a conventional EBPR system.

### 3.4. Third experimental phase (light assessment and optimization)

The reactor performance for different light intensities is shown in Fig. 8. Three of the four light intensities tested were higher than the model estimated light requirement for photosynthesis (145  $\mu\text{mol m}^{-2} \text{sec}^{-1}$ ). The oxygen production rate by microalgae decreased when the light intensity reduced (3.5, 2.7, 2.1, and 0.89 % saturated  $\text{DO min}^{-1}$  for light intensities of 350, 262.5, 175, and 87.5  $\mu\text{mol m}^{-2} \text{sec}^{-1}$ , respectively; linear correlation:  $R=0.99$ ; Fig. 8). Yet, the overall performance between light intensities was not significant ( $p > 0.05$ ). No significant variation was observed in the reactor performance regarding P release and P uptake (Fig. 8), suggesting that the culture selected in P2 conditions was resilient to inhibition by lower light intensities.

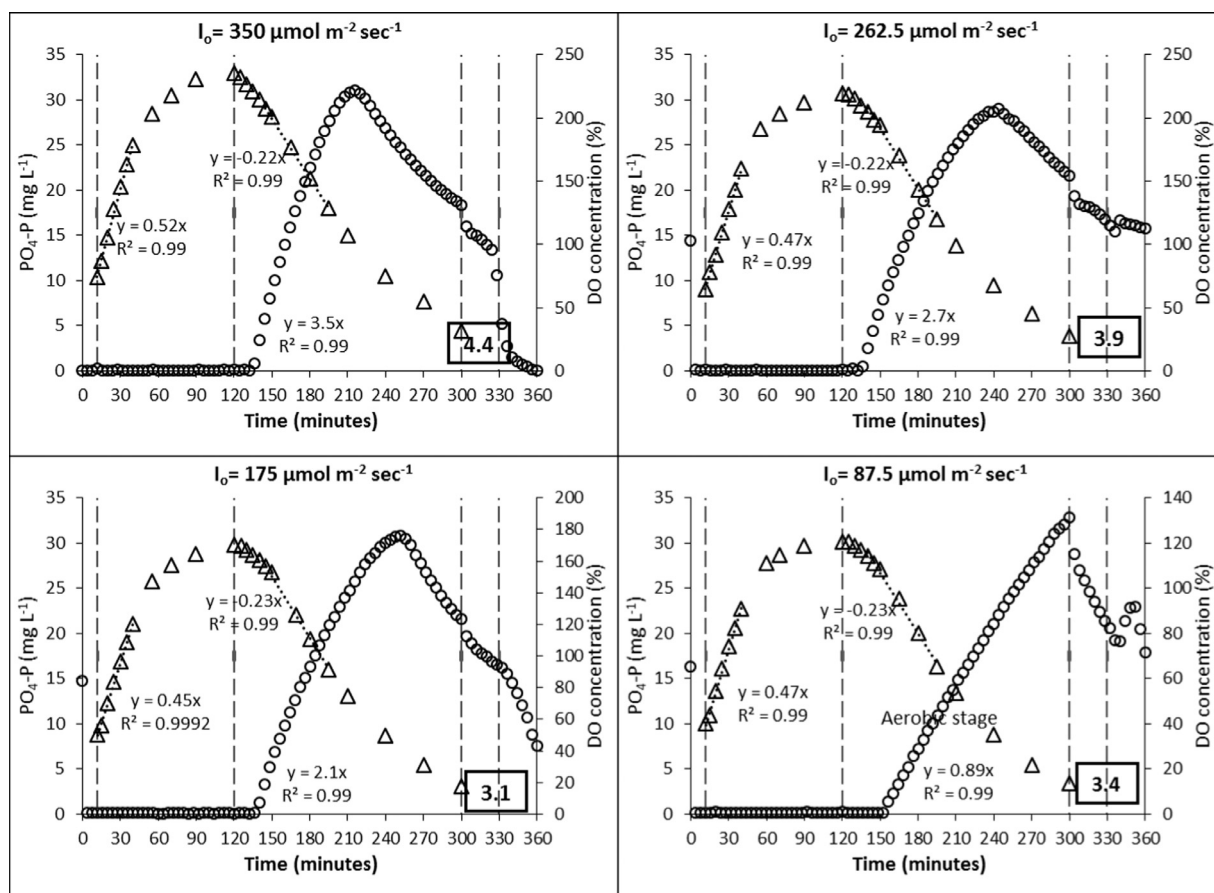


**Fig. 8.**  $\text{PO}_4\text{-P}$  profiles ( $\Delta$ ) combined with online DO profiles (o) for incident light intensities: 350, 262.5, 175, and  $87.5 \mu\text{mol m}^{-2} \text{sec}^{-1}$  for R1 on days: 83, 86, 89 and 92 of operation, respectively.

Reducing the light in P1 (e.g. from  $350$  to  $87.5 \mu\text{mol m}^{-2} \text{sec}^{-1}$ ) may limit the microalgae growth without the need to reduce the inorganic carbon as implemented in P2. This measure would possibly reduce the uptake rate of  $\text{NH}_4\text{-N}$  by microalgae (and therefore delay the early consumption of  $\text{NH}_4\text{-N}$  that occurred in P1). As the light intensity was decreased, the P concentration in the effluent improved slightly (Fig. 8). [Carvalho et al. \(2014b\)](#) observed that PAOs in an EBPR system prefer to grow in low DO concentration, and outnumber GAOs. Therefore, too much light may not be beneficial for PAOs. Conversely, too little light may also not be favourable for PAOs, as the total oxygen produced by microalgae may not meet the metabolic and anabolic requirement of PAOs as explained by the model of [Smolders et al. \(1994b\)](#).

### 3.5. Limitations and implications of the study

An EBPR-PAS system exploits the synergistic relationship between microalgae and PAOs. Uncoupling HRT from SRT facilitates the use of a smaller sized system (HRT = 12 h) than other microalgal-bacterial systems (commonly 2-6 days for municipal wastewater; [Muñoz and Guieysse, 2006](#); [Anbalagan et al. 2016](#)). Also, the EBPR-PAS system requires no external aeration, has a high capacity to remove P at low influent COD concentrations, and significantly reduces  $\text{CO}_2$  footprint. However, the current study showed that the system is not always successful and its performance depends on the composition of the influent wastewater. This may have practical implications that are difficult to discern at full-scale with real wastewater applications. For example, municipal wastewater will demonstrate an intrinsic temporal variability

([Metcalf and Eddy, 2003](#)), while the system described in our study treated wastewater at a steady  $\text{COD}:\text{HCO}_3:\text{NH}_4\text{-N}$  ratio of 10:10:4.

The current study was operated without nitrification. Introducing nitrifiers in the EBPR-PAS system has different implications. The system will require more  $\text{O}_2$  as nitrification usually demands intensive aeration ( $4.57 \text{ mg O}_2 \text{ mg}^{-1} \text{ NH}_4\text{-N}$  nitrified; [Wiesmann, 1994](#)). In addition, the nitrification process consumes a considerable amount of alkalinity ( $8.71 \text{ mg HCO}_3 \text{ mg}^{-1} \text{ NH}_4\text{-N}$  nitrified; [Wiesmann, 1994](#)), therefore, the system will require more  $\text{HCO}_3$  to produce more  $\text{O}_2$  and to meet this demand. However, denitrification can recover half the  $\text{O}_2$  and alkalinity lost in nitrification ( $2.86 \text{ mg O}_2 \text{ mg}^{-1} \text{ NO}_3\text{-N}$  de-nitrified;  $4.36 \text{ mg HCO}_3 \text{ mg}^{-1} \text{ NO}_3\text{-N}$  de-nitrified; [Wiesmann, 1994](#)). Some PAOs are assumed to use nitrate as an external electron acceptor, allowing efficient integration of simultaneous nitrogen and phosphate removal with minimal organic carbon (COD) requirements ([Sorm et al., 1996](#); [Saad et al., 2016](#)). Overall, less organic carbon, more nitrogen, and more inorganic carbon are expected for PAOs-microalgae-nitrifier symbiosis than PAOs-microalgae symbiosis.

The EBPR-PAS system in this study favored P removal even at low light intensities, which is an indication that the system can be operated at low power consumption if artificial lighting is used. However, when nitrification is incorporated in the EBPR-PAS system, more light is expected to be required by microalgae to meet the high DO demand by nitrifiers. In addition, further light is required as a result of increased TSS concentration caused by the additional biomass of nitrifiers, although the additional biomass will be minimal as nitrifiers have a very small yield ( $0.1 \text{ mg VSS mg}^{-1} \text{ NH}_4\text{-N}$ ; [Ekama and Wentzel, 2008](#)). The light path and culture den-

sity (as controlled by SRT) are potential controls to manipulate the photo-oxygenation rate (Arashiro et al., 2017; Rada-Ariza et al., 2019). For example, decreasing the light path and reducing SRT can maximize the DO concentration in the system.

#### 4. Conclusion

This study showed that careful control of  $\text{NH}_4\text{-N}$  and  $\text{HCO}_3^-$  is critical to balancing PAOs and microalgae populations in the EBPR-PAS system. At a COD: $\text{HCO}_3^-$ : $\text{NH}_4\text{-N}$  ratio of 10:20:1, the EBPR-PAS system favored nitrogen removal and microalgal growth, and exhibited poor EBPR activities. At this ratio, the growth of PAOs was likely inhibited because microalgae consume ammonium earlier than PAOs during the illuminated stage of operation. However, once the COD: $\text{HCO}_3^-$ : $\text{NH}_4\text{-N}$  ratio was changed to 10:10:4, the PAOs and microalgae populations were balanced, and the system performance improved significantly to remove P. The study also revealed that there were no significant differences in the system performance for different light intensities, suggesting that the mixed culture was robust against light fluctuations. Future studies should focus on testing the EBPR-PAS system on real municipal wastewater in large volumes to demonstrate applicability of this system to full scale operations. In addition, the incorporation of nitrification and the influence of nitrate on PAOs-microalgae interplay should be investigated further. Finally, the long-term effect of light intensity should be studied to investigate the system performance for stable reactor operation.

#### Declaration of Competing Interest

The authors declare that they have no known competing financial interests or personal relationships that could have appeared to influence the work reported in this paper.

#### Acknowledgments

The authors are grateful to Nuffic for the award of Netherlands Fellowship Program (NFP) to the first author. The authors appreciate the help of technical staff: Berend Lolkema and Peter Heerings (IHE-Delft)

#### Supplementary materials

Supplementary material associated with this article can be found, in the online version, at doi:10.1016/j.watres.2020.116606.

#### References

Abouhend, AS, McNair, A, Kuo-Dahab, WC, Watt, C, Butler, CS, Milferstedt, K, Jrm, Hamelin, Seo, J, Gikonyo, GJ, El-Moselhy, KM, 2018. The oxygenic photogranule process for aeration-free wastewater treatment. *Environmental science & technology* 52, 3503–3511.

Ahmad, JSM, Cai, W, Zhao, Z, Zhang, Z, Shimizu, K, Lei, Z, Lee, D-J, 2017. Stability of algal-bacterial granules in continuous-flow reactors to treat varying strength domestic wastewater. *Bioresource technology* 244, 225–233.

Anbalagan, A, Schwede, S, Lindberg, C-F, Nehrenheim, E, 2016. Influence of hydraulic retention time on indigenous microalgae and activated sludge process. *Water research* 91, 277–284.

Anbalagan, A, Toledo-Cervantes, A, Posadas, E, Rojo, EM, Lebrero, R, González-Sánchez, A, Nehrenheim, E, Muñoz, R, 2017. Continuous photosynthetic abatement of CO<sub>2</sub> and volatile organic compounds from exhaust gas coupled to wastewater treatment: evaluation of tubular algal-bacterial photobioreactor. *Journal of CO<sub>2</sub> Utilization* 21, 353–359.

APHA, 2005. Standard methods for the examination of water and wastewater. American Public Health Association (APHA), Washington, DC, USA.

Arashiro, LT, Rada-Ariza, AM, Wang, M, Van Der Steen, P, Ergas, SJ, 2017. Modelling shortcut nitrogen removal from wastewater using an algal-bacterial consortium. *Water Science and Technology* 75, 782–792.

Bashar, R, Gungor, K, Karthikeyan, K, Barak, P, 2018. Cost effectiveness of phosphorus removal processes in municipal wastewater treatment. *Chemosphere* 197, 280–290.

Becker, EW, 1994. *Microalgae: biotechnology and microbiology*. Cambridge University Press.

Brdjanovic, D, van Loosdrecht, MC, Hooijmans, CM, Alaerts, GJ, Heijnen, JJ, 1998. Minimal aerobic sludge retention time in biological phosphorus removal systems. *Biotechnology and bioengineering* 60, 326–332.

Carvalho, M, Oehmen, A, Carvalho, G, Reis, MA, 2014a. Survival strategies of polyphosphate accumulating organisms and glycogen accumulating organisms under conditions of low organic loading. *Bioresource technology* 172, 290–296.

Carvalho, M, Oehmen, A, Carvalho, G, Eusébio, M, Reis, MA, 2014b. The impact of aeration on the competition between polyphosphate accumulating organisms and glycogen accumulating organisms. *Water research* 66, 296–307.

Carvalho, V, Freitas, E, Silva, P, Fradinho, J, Reis, M, Oehmen, A, 2018. The impact of operational strategies on the performance of a photo-EBPR system. *Water research* 129, 190–198.

Comeau, Y, Hall, K, Hancock, R, Oldham, W, 1986. Biochemical model for enhanced biological phosphorus removal. *Water Research* 20, 1511–1521.

Craggs, R, Davies-Colley, R, Tanner, C, Sukias, J, 2003. Advanced pond system: performance with high rate ponds of different depths and areas. *Water Science and Technology* 48, 259–267.

Craggs, R, Park, J, Heubeck, S, Sutherland, D, 2014. High rate algal pond systems for low-energy wastewater treatment, nutrient recovery and energy production. *New Zealand Journal of Botany* 52, 60–73.

Ekama, G, Wentzel, M, 2004. A predictive model for the reactor inorganic suspended solids concentration in activated sludge systems. *Water Research* 38, 4093–4106.

Ekama, GA, Wentzel, MC, 2008. Nitrogen removal. *Biological wastewater treatment* IWA Publishing, London, UK, pp. 87–138.

EUMETSAT (2020) [https://www.eumetsat.int/website/home/News/DAT\\_2187685.html](https://www.eumetsat.int/website/home/News/DAT_2187685.html) (May, 2020)

Henze, M, Comeau, Y, 2008. Wastewater characterization. *Biological wastewater treatment: Principles modelling and design* 33–52.

Henze M, van Loosdrecht MC, Ekama GA, Brdjanovic D (2008) *Biological wastewater treatment* IWA publishing

Ji, B, Zhang, M, Gu, J, Ma, Y, Liu, Y, 2020a. A self-sustaining synergetic microalgal-bacterial granular sludge process towards energy-efficient and environmentally sustainable municipal wastewater treatment. *Water Research*, 115884.

Ji, B, Zhang, M, Wang, L, Wang, S, Liu, Y, 2020b. Removal mechanisms of phosphorus in non-aerated microalgal-bacterial granular sludge process. *Bioresource Technology*, 123531.

Lopez-Vazquez, CM, Oehmen, A, Hooijmans, CM, Brdjanovic, D, Gijzen, HJ, Yuan, Z, van Loosdrecht, MC, 2009. Modeling the PAO-GAO competition: effects of carbon source, pH and temperature. *Water Research* 43, 450–462.

Manser, ND, Wang, M, Ergas, SJ, Mihelcic, JR, Mulder, A, van de Vossenberg, J, van Lier, JB, van der Steen, P, 2016. Biological Nitrogen Removal in a Photosequencing Batch Reactor with an Algal-Nitrifying Bacterial Consortium and Anammox Granules. *Environmental Science & Technology Letters* 3, 175–179.

Mara D (2004) *Domestic Wastewater Treatment in Developing Countries* Earthscan Metcalf and Eddy, Inc., 2003. *Wastewater engineering: treatment and reuse*, 4th ed. McGraw-Hill, New York.

Munoz, R, Guieysse, B, 2006. algal-bacterial processes for the treatment of hazardous contaminants: a review. *Water research* 40, 2799–2815.

NEN 6472 (1983) Water-Photometric determination of ammonium content Dutch Normalization Institute Delft.

NEN 6520 (1982). Water: Spectrophotometric Determination of Chlorophyll-a Content Nederlands Normalisatie-instituut, Delft, the Netherlands

Nielsen P, Daims H (2009) *FISH handbook for biological wastewater treatment* Iwa publishing

Rada-Ariza, A, Frey, D, Lopez-Vazquez, C, Van der Steen, N, Lens, P, 2019. Ammonium removal mechanisms in a microalgal-bacterial sequencing-batch photobioreactor at different solids retention times. *Algal Research* 39, 101468.

Rada-Ariza, A, Lopez-Vazquez, C, Van der Steen, N, Lens, P, 2017. Nitrification by microalgal-bacterial consortia for ammonium removal in flat panel sequencing batch photo-bioreactors. *Bioresource technology* 245, 81–89.

Rosso, D, Larson, LE, Stenstrom, MK, 2008. Aeration of large-scale municipal wastewater treatment plants: state of the art. *Water Science and Technology* 57, 973–978.

Saad, SA, Welles, L, Abbas, B, Lopez-Vazquez, CM, van Loosdrecht, MC, Brdjanovic, D, 2016. Denitrification of nitrate and nitrite by 'Candidatus Accumulibacter phosphatis' clade IC. *Water Research* 105, 97–109.

Schuler, A, Jenkins, D, Ronen, P, 2001. Microbial storage products, biomass density, and settling properties of enhanced biological phosphorus removal activated sludge. *Water science and technology* 43, 173–180.

Smolders, G, Van der Meij, J, Van Loosdrecht, M, Heijnen, J, 1994a. Model of the anaerobic metabolism of the biological phosphorus removal process: stoichiometry and pH influence. *Biotechnology and bioengineering* 43, 461–470.

Smolders, G, Van der Meij, J, Van Loosdrecht, M, Heijnen, J, 1994b. Stoichiometric model of the aerobic metabolism of the biological phosphorus removal process. *Biotechnology and bioengineering* 44, 837–848.

Sorm, R, Bortone, G, Saltarelli, R, Jenicek, P, Wanner, J, Tilche, A, 1996. Phosphate uptake under anoxic conditions and fixed-film nitrification in nutrient removal activated sludge system. *Water Research* 30, 1573–1584.

Sutherland, DL, Turnbull, MH, Broady, PA, Craggs, RJ, 2014. Effects of two different nutrient loads on microalgal production, nutrient removal and photosynthetic efficiency in pilot-scale wastewater high rate algal ponds. *Water research* 66, 53–62.

Swinehart, DF, 1962. The beer-lambert law. *Journal of chemical education* 39, 333.

van der Steen, P, Rahsilawati, K, Rada-Ariza, AM, Lopez-Vazquez, CM, Lens, PN, 2015.

- A new photo-activated sludge system for nitrification by an algal-bacterial consortium in a photo-bioreactor with biomass recycle. *Water Science and Technology* 72, 443–450.
- van Loosdrecht MC, Nielsen PH, Lopez-Vazquez CM, Brdjanovic D (2016) *Experimental methods in wastewater treatment* IWA publishing
- Welles, L, Abbas, B, Sorokin, D, Lopez-Vazquez, C, Hooijmans, C, van Loosdrecht, M, Brdjanovic, D, 2017. Metabolic Response of "Candidatus Accumulibacter Phosphatis" Clade II C to Changes in Influent P/C Ratio. *Front Microbiol* 7, 2121 103389/fmicb.
- Welles, L, Tian, W, Saad, S, Abbas, B, Lopez-Vazquez, C, Hooijmans, C, van Loosdrecht, M, Brdjanovic, D, 2015. Accumulibacter clades Type I and II performing kinetically different glycogen-accumulating organisms metabolisms for anaerobic substrate uptake. *Water research* 83, 354–366.
- Wentzel, MC, Comeau, Y, Ekama, GA, van Loosdrecht, MC, Brdjanovic, D, 2008. Enhanced biological phosphorus removal. In: Henze, Mogens (Ed.), *Biological Wastewater Treatment-Principles, Modelling and Design*, pp. 155–220.
- Wentzel, M, Ekama, G, Dold, P, Marais, G, 1990. Biological excess phosphorus removal-steady state process design. *Water Sa* 16, 29–48.
- Wiesmann U (1994) *Biological nitrogen removal from wastewater* Biotechnics/wastewater:113-154.
- Wilderer, PA, Irvine, RL, Goronszy, MC, 2001. *Sequencing batch reactor technology*. IWA publishing.